3D Printing of Bone Material Scaffolds to Improve and Replace Traditional Human Bone Implants

By Will Glockner, Gabrielle Munoz, Kahler Newsham
Tufts University
BME-153 Paper
Professor Grasman
10 December 2018

Authorship Page

All authors contributed equally to the writing and editing of this paper.

Will Glockner

Gabrielle Munoz

Kahler Newsham

1. Summary / Abstract

Approximately 95,000 bone graft surgeries are performed per year in the United States. These bone graft surgeries are used as a form of treatment in injuries including fractures, joint pathology, infections that can cause bone loss, and in implanted medical devices. While an autologous graft is currently the standard of care, it is not always possible when the patient cannot withstand another surgery to take out the graft sample. For this reason, the use of synthetic bone graft materials has increased by about 5% over the past 15 years (Kinaci et al., 2014).

An increase in the use of synthetic bone implants in recent years has also been tied to the demand for precise, custom-fit implants. 3D printing allows for precise control of scaffold size, shape, and pore size and interconnectivity while maintaining the ability for post-printing modification. A scaffold for osteogenic implementation should have a degradation profile that allows for continued support of the existing bone while slowly being replaced by new bone growth. To achieve this balance, we will investigate varying composite ratios of poly(lactide-co-glycolic acid) (PLGA) and poly(epsilon-caprolactone) (PCL) in a 3D printed scaffold. As with any invasive procedure, there is a risk of infection; however, in bone tissue, microbes will induce additional acute inflammation which may lead to necrosis and thus a diminished efficacy of antibiotic treatment due to decreased vascularization. This may lead to the development of a biofilm and thus the need for additional surgery. In fact, the rate of infection in bone graft surgeries has been reported to be between 3 - 12 % of all bone graft operations (Lee et al., 2015).

To address this concern, we will investigate the modification of our materials with antimicrobial peptides (AMPs). We will analyze the efficacy of the attachment of Magainin II in varying concentration ratios on all PLGA/PCL composite scaffolds produced and analyze the efficacy of Magainin II *in vitro* and *in vivo*. This analysis will include proliferation, metabolic, and minerizational assays as well as morphological observations. The most effective materials will be selected for musine *in vivo* studies. First, further cytotoxic and biocompatibility test will be performed to confirm *in vitro* findings. This will be followed by tests to determine the efficacy of the scaffolds to repair an induced bone defect as well as bacterial quantification. At the conclusion of our experiments, we will have determined which PLGA/PCL composites represent the best degradation profiles, are amenable to AMP modification, are biocompatible, promote cell attachment, and support the growth of bone after implantation. It is expected that the scaffolds with higher concentrations of PLGA than PCL, and a Maginin II concentration of 0.025 mg ml^{-1} will give the best *in vivo* response, and support the regeneration of bone material.

2. Specific Aims

About 95,000 bone graft surgeries are performed annually in the US for various injuries, illnesses, and medical devices. But in recent years, the need for synthetic grafts has increased from about 15% of bone grafts to 20%. One issue with synthetic grafts is infection, with an infection rate between 3 - 12 %. This paper aims to develop a 3D printed composite material, to manipulate the properties of PLGA and PCL to support bone regeneration, with Maginin II affixed to the composite scaffolds to combat infection in an *in vivo* environment. This objective will be achieved through the following aims.

Specific Aim #1: Identify PLGA/PCL Composite Materials Most Similar to Bone

First, we aim to develop a 3D printed PLGA/PCL composite. Composite scaffolds will be printed using Fused Deposition Modeling (FDM), and characterized using SEM (for porosity, uniformity, and interconnectivity), a tensile test, a degradation test, and a biocompatibility test. It is hypothesized that FDM printing will not significantly impact the composite material properties from their natural properties. We will then select promising composite ratios to study further. PLGA and PCL printing using FDM have shown to be effective scaffolds; however, a composite material has not yet been investigated. If issues occur when printing the composite material using FDM, or the material properties differ from expected, we will examine other rapid prototyping methods (Park et al., 2012).

Specific Aim # 2: Magainin II immobilization by concentration and antibacterial resistance

We aim to determine the feasibility of immobilizing antimicrobial peptide (AMP) Magainin II on a composite scaffold and to better understand the Magainin II solution concentration needed to grant composite scaffolds antimicrobial properties. We will attempt to immobilize Magainin II on our PLGA scaffolding by EDC/NHS coupling (Yüksel et al., 2016). Scaffolds will be exposed to three levels of Magainin II solution concentration and tested for antimicrobial properties. Immobilized scaffolds will be studied though SEM, X-ray photoelectron spectroscopy, atomic force microscopy, and live/dead assays using SYTO-9 staining (Humblot et al. 2009). We hypothesize that AMPs can be successfully immobilized on the porous PLGA and PCL composites and expect the most efficacious Magainin II solution concentration will be contingent on the material properties of a composite scaffold. If we are unable to cause the EDC/NHS functionalized PLGA composite scaffolds to bond with Magainin II, our team will examine bonding microspheres containing Magainin II to our composite scaffold and examine the concentration needed for effective localized release.

Specific Aim # 3: Analysis of Biocompatibility and Osteogenic Properties in vitro *and* in vivo

Our final aim to is study our materials *in vitro* and *in vivo*. We will characterize cell metabolism, proliferation, and cytotoxicity. To test the bioinstructive capabilities of the scaffolds, we will seed the scaffolds with osteoblast cells and analyze the cells for lineage-specific markers to determine the extent of differentiation. Further, we will measure mineralization and characterize cell attachment. The materials with the best performance on the above tests will be implanted in mice after a bone deformation is made. X-ray and μCT will be used to monitor healing, and after mice are sacrificed, histological analyses will be performed to measure bone formation. The scaffolds with a combination of PLGA and PCL are expected to demonstrate the best *in vitro* results as well as the best osteogenic properties. The scaffolds containing AMPs are expected to be the most resistant to infection *in vivo*. At the conclusion of this study, scaffold compositions will be identified which promote bone regeneration and resist microbial infection.

3. Background and Significance

3.1 Current Bone Graft Market

With recent advances in technology and medicine, the ability to fix more illnesses and medical problem has become possible. Thus, the need for bone grafts has risen as the number of procedures that require bone grafts has increased. In fact, in 2007 alone, approximately 95,000 bone graft surgeries were performed (Kinaci et al., 2014). Bone grafts are commonly used as a form of treatment in injuries including fractures, illnesses such as joint disease, infections that can cause bone loss, and in implanted medical devices. Because the need for bone grafts are so widespread, there are many different types of bone grafts, depending on the application. These types include human grafts, both allografts from a donor, and autografts from the patient, and synthetic grafts. These different types of grafts can be tailored for the individual patient.

Recently however, patients have been shifting towards a higher use of synthetic bone grafts. In fact, from 1992-1995, roughly 15% of bone grafts implanted into patients were synthetic grafts, but from 2004-2007, roughly 20% of bone grafts implanted into patients were synthetic grafts (Kinaci et al., 2014). This trend demonstrates that the demand for synthetic grafts will likely increase. While native bone is almost always a superior material for bone grafts, it is not always available and it must be a physical and cellular match to the tissue it is replacing. Moreover, allografts from a different donor offer a risk for rejection and infection, are limited in availability, and may not match the shape or need as well. Synthetic grafts can be used to easily create a standard and well-characterized graft material that can be used for a variety of different patient needs when autografts or allografts are not possible.

Current synthetic grafts are made from a variety of polyester or polyester composite materials, and created to match the shape of a specific injury. However, these shapes do not always match the needs of the patient, and may require additional processing and time to fit the patient need. With the advances of 3D printing though, a scaffold can be printed to match the exact need of a patient, depending on the exact defect. There are currently many methods of 3D printing, but fused deposition modeling (FDM), has been used to successfully print scaffolds for tissue engineering in many applications.

Table 1. Summary of Current Bone Graft Options

Graft Type *Description*	Advantages	Disadvantages
Allografts *Natural grafts from a different donor*	-biocompatible -natural material	-risk of rejection -risk of infection -limited availability -may not match patient need (shape or biological match)
Autografts *Natural grafts from the patient*	-biocompatible -natural material -perfect match to patient (low risk of rejection)	-requires additional surgery -material may need to be further processed to create the graft fit

Synthetic Grafts *Grafts made chemically in a lab*	-chemically tunable -well-characterized -standardized and repeatable -range of possible shapes and materials	-not a natural material -risk of rejection -risk of infection / irritation -expensive

Table 1 summarizes the advantages and disadvantages of current bone grafts options

3.2 3D Printing Methods

FDM is an advantageous 3D printing method because it is a fast and inexpensive method of printing. It is used to melt the desired material down and extrude it into the desired shape layer by layer. FDM allows for a high level of control on the shape and interconnectivity of the scaffold being printed, through the CAD design inputted into the printer. FDM has been used to successfully print both PLGA and PCL scaffolds. However, the composite material has not yet been studied (Park et al., 2012). It is desirable to use both PLGA and PCL for their biocompatibility and controllable degradation profiles. By testing composite ratios of both materials, it may be possible to mimic natural bone material more accurately than with a single material.

3.3 PLGA and PCL Materials

A material that mimics natural bone material can be designed from both PLGA and PCL. This material must be biocompatible, have a controllable degradation rate, be mechanically strong, porous, and able to support cellular regeneration. Because PLGA and PCL are both biocompatible and have controllable degradation rates, the composites of these materials can be studied to create a material that best matches the porosity and strength of natural bone material. It is important to test these properties after they have been 3D printed into the scaffolds, as the high printing temperature may impact some of the properties of the materials, along with the new composite ratios of the material.

3.4 Bacterial Infections with Grafts

Bacterial infection is one of the most dangerous complications that can occur with invasive surgery and implanted biomaterials. This is because bacteria can group together and form a unique and complex microbial community that is called a biofilm. (Costerton et al., 1987). This biofilm frequently requires the removal of an implant which can lead to prolonged hospital time and increased risk of scarring associated with surgical revisions (Costa et al., 2011). Biofilms are especially dangerous as they offer a degree of resistance to antibiotics and disinfectants making them incredibly resistant to bacteria (Donlan et al., 2002). It has been found that established biofilms can survive antimicrobial agents at 10 to 1,000 times higher than the concentration required to kill genetically identical planktonic bacteria (Lewis et al., 2001).

3.5 Antimicrobial Peptides

In order to combat these biofilms, research has been conducted on release antibiotics and antimicrobial heavy metals like silver (Liu et al., 2012) (Qi et al., 2013). Although these methods to combat biofilms have demonstrated some efficacy, increasing concerns around

antibacterial resistance and toxic side effects have prompted researchers to explore new methods to combat biofilms. Consequently, recent research has been investigating antimicrobial peptides (AMPs). AMPs can offer broad-spectrum activity and some AMPs have the ability to kill off antibacterial resistant bacteria.

AMPs offer an alternative to some metals and some standard antibiotics. One of the key advantages is that they offer efficacy at very low concentrations (Costa et al., 2011). This means that some AMPs may be used in a fashion that delays the development of bacterial resistance. Some AMPs are part of the immune system and are secreted by animals, plants, and other microorganisms to fend off bacteria. The physicochemical properties allow some AMPs to interact with negatively charged microbial membranes (Costa et al., 2011). Although the methodology of providing antibacterial resistance varies depending upon the AMP in question, a large percentage of AMPs use physical properties to destroy bacteria. Some AMPs pierce through the bacteria cell membrane and, through this action, induce a cytoplasmic implosion and corresponding lysis of bacterial cells.

This paper will largely cover the AMP Magainin II (Mag II). Mag II is a 23-residue AMP that will be immobilized on our PLGA & PCL scaffolds via covalent binding. This binding is accomplished using EDC/NHS coupling(Nie et al., 2009). Past research has successfully investigated the antimicrobial properties of Mag II on electrospun PLGA and found that covalently immobilized Mag II offered electrospun PLGA increased antibiotic resistance (Yüskel et al., 2014).

This experiment will be determined to be a success if our team is able to demonstrate that Mag II is a viable surface modification for 3D printed PLGA and PCL scaffolds. At a macro level, these findings could pave the way for a new generation of implants that offer an incredible degree of customization for bone replacement. The importance of a highly adaptable biomaterial with an ingrained capacity for antimicrobial behavior is novel. These findings could help direct the development of future implants as well as offering further research into the capacity of AMPs as antibacterial resistance becomes a mounting concern to the scientific and medical community.

4. Research Design and Methods

4.1 Specific Aim # 1: Identify PLGA/PCL Composite Materials Most Similar to Bone

4.1.1 Introduction

The objective of the first aim is to determine the optimal scaffold material, from a range of PLGA and PCL composites. After a range of composites have been studied, those that show promising results will be examined further for this application. Both materials are used widely in tissue engineering, for their biocompatibility, strength, and controllable degradation rate. However, a composite material has not yet been 3D printed successfully for this application. A composite material may be desirable to further manipulate the different properties of these materials including degradation, porosity, and strength. However, 3D printing the materials together may impact and change their physical properties, so the scaffolds need to be fully characterized before they can be studied for further applications.

For this aim, the pure 3D printed PLGA and PCL scaffolds will serve as the controls for comparison. From the range of composites, it is first necessary to see if the FDM 3D printing method impacts the scaffold properties at all. Then, it is desired to find the composite ranges that have the longest degradation times that can support cell regrowth for the longest time, and have a similar strength and porosity to the natural bone material. Finally, the biocompatibility of the scaffolds will be studied, to ensure that the material is a viable clinical option. Because these are all important scaffold properties, all of these properties will be weighed when choosing promising composite ratios to pursue further.

4.1.2 Composite Scaffold Printing

PLGA and PCL composite scaffolds will be 3D printed using fused deposition modeling (FDM). Specifically, ratios of 0:100, 20:80, 40:60, 50:50, 60:40, 80:20, 100:0 of PLGA to PCL will be printed and studied. While PLGA and PCL have very different properties, including glass transition temperature and melting temperature, the materials will be mixed together directly in the specified ratio, and printed at a single set of conditions. Because the FDM printing process has already been optimized for both PLGA and PCL independently, the composite scaffolds will be printed between the optimal conditions for both materials as described next. The scaffolds will be printed with a nozzle tip inner diameter of 0.01 mm, at a liquefier temperature of 125°C, and at a roller speed of 0.08 rps, all while the environmental temperature is maintained at 25°C. The scaffolds will be printed into 12 mm diameter films, that are 2 mm thick, which will be designed in SolidWorks. These scaffolds will also be designed with a porosity between 75 - 85 %, with 300-600 um diameter pores. After printing, the scaffolds will be stored in a dessicator (Zein et al., 2002).

Figure 1. Structure of Cancellous Bone

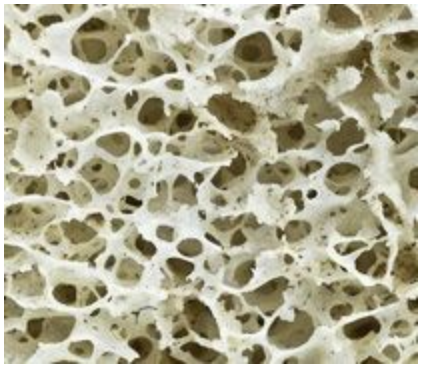

Figure 1 shows the natural structure of cancellous bone that will be attempted to be replicated during scaffold design in SolidWorks ("Bone Anatomy", 2011).

4.1.3 Scaffold Characterization

After printing, all composite ratios of the scaffolds will be characterized through scanning electron microscopy (SEM), to evaluate the pore size, interconnectivity, and uniformity of the FDM printed scaffolds. Both dry scaffolds, and wet scaffolds that have been immersed in 15 mL phosphate buffered solution (PBS) for 30 min, will be examined by SEM to compare the wet and dry scaffold properties (including porosity, interconnectivity, and uniformity), and ensure that hydration of the scaffolds does not significantly change their properties. This test will be used to determine the composite materials that show the best porosity and uniformity, similar to natural bone material.

4.1.4 Mechanical Test

A stress / strain test will be used to compare the strength of each composite scaffold. Each scaffold will be uniaxially compressed at a rate of 2 mm/min. These compressive tests will be run at 37°C. Deformation can be measured in terms of compression ratio, as well as strain, which can be used to create a stress / strain curve for each material, and calculate the Young's modulus for each composite. These tests will be performed on both dry scaffolds, and wet scaffolds that have been immersed in 15 mL PBS for 30 min, to compare the wet and dry properties of the scaffolds and ensure that the *in vivo* environment will not significantly change the scaffold properties (Martín et al., 2017). For this test, the pure PLGA and PCL scaffolds (both wet and dry) will serve as controls for the composite ratios. This test is important to ensure that the scaffolds will be strong enough to support extended cell regrowth and bone functions.

4.1.5 Degradation Test

The degradation of each composite scaffold will be studied. Each scaffold will be submerged in 15 mL PBS, at 37°C. This temperature was chosen to mimic *in vivo* conditions, because it is the average body temperature. The time it takes for each scaffold to fully dissolve will be measured. Moreover, the pH of each PBS solution will be measured every 2 days until each scaffold has fully dissolved. To simulate *in vivo* conditions, degradation will also be studied under sink conditions. This will be used to simulate product clearance through diffusion. In

this degradation study, each scaffold will again be submerged in 15 mL PBS, at 37°C, but the PBS will now be replaced with new PBS every 7 days. Again the time it takes for each scaffold to dissolve will be measured, and the pH of each solution will be measured before it is replaced with new PBS. The pH change over each PBS media change will be measured, because cumulative pH change can no longer be measured (Xu et al., 2018). The timepoints in these tests were arbitrarily chosen; however, if the scaffolds are showing faster or slower degradation, the measurement timepoints will be adjusted. This test determines which scaffolds have the most optimal degradation profiles for supporting cell regrowth over longer periods of time, and ensures that degradation does not change significantly in *in vitro* and *in vivo* environments.

4.1.6 Biocompatibility Study

After all the composite scaffolds have been characterized, they will be investigated for their biocompatibility. These materials will be implanted into mice subcutaneously and studied. After 30 days, histological samples will be taken and analyzed for the presence of multinucleated giant cells as an indication of a foreign body response. (Al-Maawi et al., 2017) If needed, materials that are not compatible *in vivo* will not be used in further experiments.

4.1.7 Expected Outcomes

It is expected that FDM printing of the composite materials will not significantly impact the material properties. First, it is expected to see a precisely controlled pore size, interconnectivity, and uniformity between all scaffolds. It is also expected that scaffolds with more PCL will be stronger than scaffolds with more PLGA. Moreover, it is expected that the scaffolds with more PLGA will degrade faster than the scaffolds with more PCL. Finally, it is expected that all composites will be biocompatible options. These expectations were made from existing PLGA and PCL or composite properties, but not from the properties of the 3D printed materials. It is also expected that the properties of the dry scaffolds, such strength and porosity, will not change significantly when they are hydrated.

4.1.8 Alternative Directions

Because PLGA and PCL composites have not yet been studied by FDM printing, it is important to acknowledge alternative directions. If issues occur when printing the composite material using FDM or if material properties differ dramatically from expected values in the form of the pure control scaffolds, we will examine other rapid prototyping methods, such as inkjet bioprinting, selective laser sintering, and powder 3D printing (Jariwala et al., 2015). Moreover, the running conditions of the FDM printing can be further optimized to the individual scaffold ratios if necessary.

4.2 Specific Aim # 2: Determine Magainin II solution that optimizes antibacterial resistance

4.2.1 Introduction

The goal of the second aim is to determine which concentration of Magainin II solution is most effective at granting antibacterial properties to a PLGA and PCL composite scaffold. After observing which level of Magainin II concentration optimizes antibacterial properties, the most efficacious concentration will be documented and used in biocompatibility trials. Although

there is existing research on immobilizing Magainin II on PLGA, this experiment will further explore the relationship between Magainin II solution concentration and amount of Magainin II immobilized.

In this aim, researchers will use an untreated scaffold as a negative control and compare microbial growth on this untreated scaffold to all Magainin II affixed trials. Researchers expect that Magainin II grafting will be successful at all concentrations and, to confirm this, we will compare each trials antibacterial properties to the untreated scaffold. In addition to comparing each trial to the negative control, researchers will investigate the differences in antimicrobial behavior exhibited between scaffolds where Magainin II was immobilized at different concentrations. From this research, we hope to display which concentration of Magainin II solution yields the most effective antimicrobial response.

4.2.2 Materials

The most optimal PLGA and PCL scaffold, as determined in specific aim 1, will be used for all trials of the AMP Magainin II (Mag II) immobilization. In order to execute EDC/NHS coupling our research group will purchase the following: 1-ethyl-3-(3-dimethylaminopropyl)-carbodiimide hydrochloride (EDC), N-hydroxysuccinimide (NHS), mess buffer solution, and phosphate buffered saline tablets (Yüksel et al., 2016). To assess the amount of bacterial growth on scaffolds, researchers will purchase and use the LIVE/DEAD Bacterial Viability Kit (BacLight^{TM}) (Humblot et al. 2009).

4.2.3 Magainin II immobilization

The Antimicrobial peptide Magainin II (Mag II) will be covalently immobilized on the scaffolds through through EDC/NHS coupling. The scaffolds will be placed in a solution containing EDC (10 mM) and NHS (10 mM) in 0.1M MES solution for five hours (Yüksel et al., 2016). The scaffolds will then be exposed to three concentrations of Mag II solution(0.010 mg ml^{-1}, 0.025 mg ml^{-1}, and 0.040 mg ml^{-1}). A scaffold will be placed in each of these Mag II solutions and subsequently combined with a phosphate buffer. The immersed scaffolds will then be incubated at room temperature for 12 hours. After undergoing this treatment, the scaffolds will be washed with DI water, dried, and then stored in refrigerated conditions (4° C).

Figure 2. Binding Mag II to PLGA

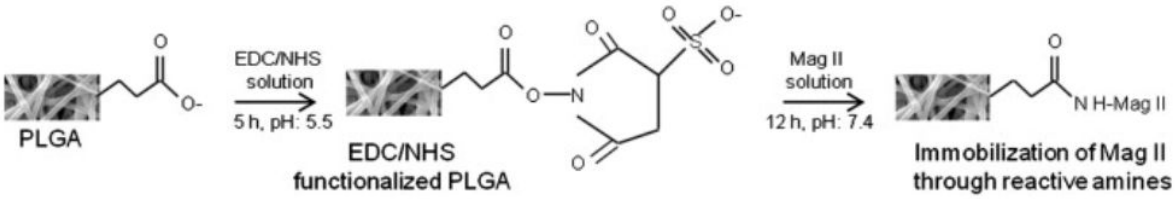

*Figure 2 shows the process by which Maganin II can be immobilized upon PLGA (*Yüksel et al., 2016)

4.2.4 Confirmation of Mechanical Properties

After every scaffold has been loaded from different concentrations of Mag II solution, the scaffolds (PLGA-PCL-MagII.010, PLGA-PCL-MagII.025, and PLGA-PCL-MagII.040) will undergo the mechanical tests previously outlined in 4.1.5 and 4.1.4. This repetition is included in order to determine if the procedure for immobilizing Mag II has changed the structural properties of the scaffold.

4.2.5 Scanning Electron Microscopy (SEM)

The morphologies of our scaffolds (PLGA-PCL hybrid, PLGA-PCL-MagII.010, PLGA-PCL-MagII.025, and PLGA-PCL-MagII.040) will be observed using a scanning electron microscope at a voltage range of 5 to 20 kV. All samples will be sputter coated to prevent the charging of the specimen from the accumulation of static electric fields to increase our signal to noise ratio. As of now, researchers intend to use a gold-palladium hybrid for the sputter coating.

4.2.6 X-ray Photoelectron Spectroscopy (XPS)

The surface chemical composition of all FDM printed scaffolds (PLGA-PCL hybrid, PLGA-PCL-MagII.010, PLGA-PCL-MagII.025, and PLGA-PCL-MagII.040) will be observed using X-ray Photoelectron Spectroscopy (XPS). XPS is a spectroscopic technique that allows researchers to understand what elements are within a layer of a given sample and provides information about what the elements are bonded to. Consequently, data surrounding the energy states of carbon, oxygen, and nitrogen on the scaffolds surfaces will help model the extent of Mag II immobilization that has occured on a given scaffold. For this experiment, the pressure will be kept at below 10 Torr with 20 eV for a scan at a takeoff angle of 45° (Yüksel et al., 2014).

4.2.7 Atomic Force Microscopy (AFM)

The topography of our scaffolds (PLGA-PCL hybrid, PLGA-PCL-MagII.010, PLGA-PCL-MagII.025, and PLGA-PCL-MagII.040) will be measured with AFM before and after the Mag II immobilization to measure if contact has been made. The AFM images will be at room temperature in both conditions. Also, in both cases the AFM will use a silicon tip.

4.2.8 Measuring antibacterial properties of scaffold with Magainin II

To test the efficacy of the AMP Mag II surface modification, scientists will test the ability of Escherichia coli (E. coli) and Staphylococcus aureus (S. aureus) to grow and thrive on all scaffolds (PLGA-PCL hybrid, PLGA-PCL-MagII.010, PLGA-PCL-MagII.025, and PLGA-PCL-MagII.040). To measure bacterial cell adhesion, each scaffold will be placed in a solution that will be sterilized by exposure to UV radiation. Scaffolds will be immersed in this sterilized solution and seeded with either E. coli or S. aureus. The scaffolds will then be incubated for 6 hours at body temperature (37°C). In order to remove loosely adhered bacteria, the scaffolds will be washed with a sterilized phosphate buffer solution. After this rinse is complete, an SEM at an accelerating voltage of 5-20 kV will be used to measure the amount of

adhered bacteria on each scaffold (PLGA-PCL hybrid, PLGA-PCL-MagII.010, PLGA-PCL-MagII.025, and PLGA-PCL-MagII.040)(Yüksel et al., 2016).

To ensure that we are not mistakenly categorizing bacterial cells that are dead, our team will perform a live/dead assay procured from BacLight. All scaffolds, will be washed in a sterile 0.9% NaCl solution to remove bacteria that are not affixed to our them. The team will then place scaffolds in the SYTO 9 staining solution (25°C, 20 min) (Yüksel et al., 2016). After this treatment, stained bacteria will be studied under a confocal microscope to look for viability of bacteria on scaffolds modified by Mag II. Researchers believe that a live/dead assay is sufficient to model bacteria death as this segment of the experiment is acellular. If future iterations of this experiment want to examine cellular modifications in addition to the amp Mag II, more targeted assays could be used to ensure only bacterial cells are quantified. However, in the absence of any other cells, researchers believe a live/dead assay will accurately characterize the population of bacteria on all scaffolds. Researchers will quantify this growth and compare results from all scaffolds.

4.2.9 Expected Outcomes

Researchers expect that all scaffolds with functionalized Mag II will exhibit a higher degree of antimicrobial behavior than the negative control. Of the the scaffolds with functionalized Mag II (PLGA-PCL-MagII.010, PLGA-PCL-MagII.025, and PLGA-PCL-MagII.040), our team expects that the surface area of the FDM composite scaffold and its material composition will play a key role in determining which concentration of Mag II is best. Since researchers are aware that the material best suited for FDM will govern the properties needed to predict which concentration will display sufficient efficacy, we will refrain from placing a direct hypothesis and, instead, offer a ruleset for behavior we expect to see. The guidelines for our expectations are as follows: If the best composite is composed of more PLGA than PCL the higher concentrations of Mag II will be favored due to a higher presence of bonding sites. The contrapositive suggests that if there is a higher amount of PCL than PLGA, lower concentrations of Mag II in a solution would be needed to display efficacy. If FDM scaffolds offer low porosity and low surface area, lower concentrations of Mag II will be required. If FDM scaffolds are characterized as intensely porous, higher concentrations of Mag II will display enhanced antimicrobial behavior.

4.2.10 Alternative Directions

If the Mag II cannot be grafted onto our PLGA-PCL scaffolds, we will pursue attaching PLGA microspheres that encapsulate AMPs to scaffolds. There is increasing amounts of literature suggesting that AMPs can be loaded on PLGA/chitosan microspheres (Li et al., 2017). We would choose to examine this if we are unable to covalently immobilize Mag II on scaffolds. Microspheres will be pursued as they can offer localized release of AMPs, like Mag II, with a predictable degradation rate.

4.3 Specific Aim # 3: Analysis of Biocompatibility and Osteogenic Properties *in vitro* and *in vivo*

4.3.1 Introduction

The goal of the third aim is to characterize our materials both *in vitro* and *in vivo*. In order to do this, materials that showed promising results in previous characterizations will be selected. These materials will be seeded with human osteoblast cells and their metabolism, proliferation, cytotoxicity, differentiation, and mineralization will be evaluated. Fluorescence microscopy will be used to characterize initial cell attachment. After these analyses, further selection of materials may be performed. Finally, a radial bone defect will be produced in mice and a printed scaffold will be inserted. Mouse antibody titers to both *Escherichia coli* and *Staphylococcus aureus* as well as bone volume will be monitored closely. After sacrificing the animals, histological analyses and bacterial quantification will be performed.

4.3.2 Cell metabolism, Proliferation, and Cytotoxicity Analysis

$5x10^6$ osteoblasts will be seeded on scaffolds of $1cm^3$ in size. After one week of incubation scaffolds will be analyzed. A MTT assay will be used to measure cell metabolism and indicate cell viability. This will be further characterized using a fluorescent dsDNA assay to give real-time data regarding cell death and cell viability. An increase in fluorescent signals correlates with cell death and results can be made relative to negative controls in which no cells were seeded onto the scaffold. (Chiaraviglio et al., 2014)

4.3.3 Differentiation and Mineralization Assays

$5x10^6$ osteogenic cells will be seeded on scaffolds of $1cm^3$ in size and incubated for 7, 15, or 30 days. Following this, q-RT-PCR will be used to measure the expression of genes associated with osteoblast differentiation such as osteocalcin, Runx2, and osteopontin. (Wang et al., 2015) Similarly, an alizarin red assay and von Kossa staining will be used to measure calcification and mineralization in the scaffolds 7 days, 15 days, and 30 days after cell seeding. These time points have previously been shown to be sufficient to characterize PLGA scaffolds (Fu et al., 2017).

4.3.4 Fluorescence Microscopy

GFP-positive osteoblast cells will be used to visualize cell attachment, spreading, and morphology 1 hour, 6 hours, 12 hours, and 24 hours after cell seeding. Scaffolds both with and without AMPs will be analyzed to determine if the addition of AMPs affects cell attachment. Further, different biomaterial compositions will be compared to determine which material promotes the most attachment.

4.3.5 Production of Implantable Scaffold

Scaffolds of 2mm in length to correspond with the induced radial bone defect will be printed using all biomaterials that were shown to be biocompatible in *in vitro* experiments. Controls for each material will also be produced without AMP attachment to measure the antimicrobial properties of the materials. Osteoblast cells harvested from the same mouse strain should be harvested and cultured. The scaffolds will be seeded with $5x10^6$ cells (Luo et al., 2013).

4.3.6 Bone Defect Formation

For *in vivo* studies, we will use a mouse model with a humanized immune system. We will use 10 mice aged 10 weeks old per condition. First, we will anesthetize mice with isoflurane gas and then expose the radius of one paw of the mouse. Then, using a bone cutter, we will remove a segment of exactly 2mm from the radius. As previously shown, this segmental defect is

effective for testing bone regeneration as it is small enough to not heavily impact the mouse, yet large enough to be able to analyze quantitatively (Cheng et al., 2018). The bone defect will be monitored using radiography, and the weight, behavior, and movement of the mice will be monitored after surgery (Llopis-Hernandez et al., 2016).

4.3.7 Implantation of Scaffolds into Mice

After the removal of the 2mm radial bone fragment, the scaffolds seeded with human osteoblast cells will be fitted into the gap. The muscle and skin will be repositioned and the mice will be allowed to recover for eight weeks. IgM and IgG antibody titers to both *Escherichia coli* and *Staphylococcus aureus* will be measured before implantation, and 30 days, 60 days, and 90 days after implantation using a serum enzyme-linked immunosorbent assay (Kim et al., 2015).

4.3.8 Bone Formation, Histological Analyses, and Bacterial Quantification

Bone samples will be explanted and analyzed using X-ray and μCT scanning to determine the volume of new bone formation at 30 days, 60 days, 90 days, and 120 days. Mice will be sacrificed 90 days and 120 days after implantation. Histological samples will be fixed and analyzed to determine the extent of calcification and bone morphology (Cheng et al., 2018). Von Kossa staining will be used to measure mineralization and histochemical alizarin red will be used to stain for calcium. Hematoxylin will be used to stain for osteoblasts. Osteocalcin and bone sialoprotein will be used to confirm osteoblast differentiation (Bilousova et al., 2011). To quantify the bacterial count, bone tissue at the site of implantation will be collected and ground. One gram of bone powder will be resuspended in 2mL of PBS and spread on agar plates. The number of viable colonies will be counted after incubation at 37°C overnight (Nie et al., 2017).

4.3.9 Expected Outcomes

We expect to see varying cell metabolism, proliferation, cytotoxicity, and mineralization dependent on the composition of scaffolds tested. Any scaffold that produces undesirable results will not be tested *in vivo*. Similarly, we expect bone formation to vary depending on composition of the scaffold. We expect to see lower rates of infection with scaffolds produced with AMPs.

4.3.10 Alternative Directions

The characterization of scaffolds using the methods provided above has been well studied and shown to be effective. However, if the production of a 2mm scaffold size proves to be too difficult, then a larger rabbit model may be used for *in vivo* tests. If too many or too few colonies are observed when quantifying bacterial presence, the concentration of bone powder added to plated will be adjusted.

Figure 3. Process Flow Diagram

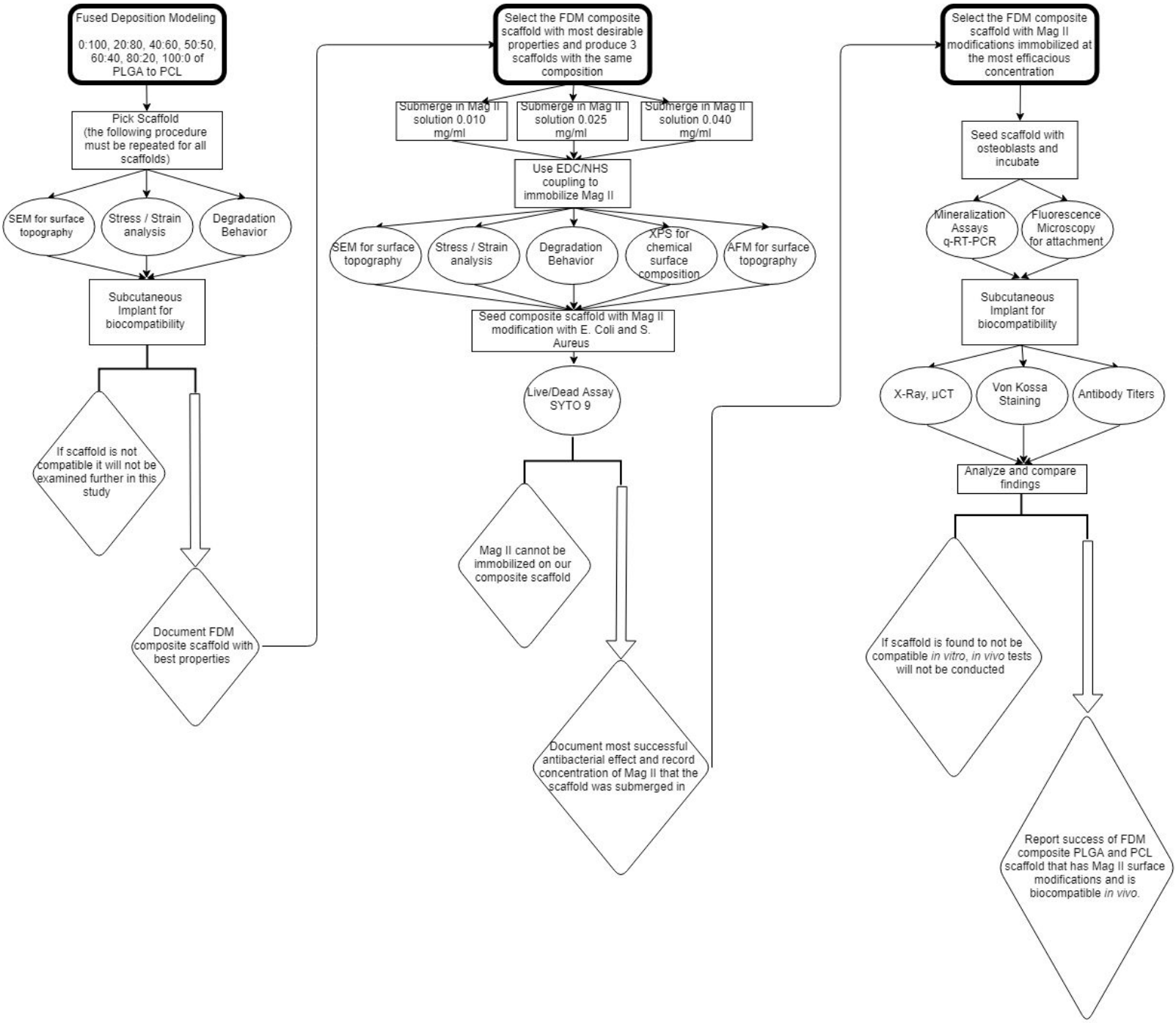

Figure 3 shows a process flow diagram for the overall project.

5. References

Al-Maawi S, Orlowska A, Sader RC, Kirkpatrick J, and Ghanaati S. In vivo cellular reactions to different biomaterials—Physiological and pathological aspects and their consequences. *Seminars in Immunology*. 2017; 29:49-61.

Bilousova G, Jun DH, King KB, De Langhe S, Chick WS, Torchia EC, Chow KS, Klemm DJ, Roop DR, Majka SM, Osteoblasts Derived from Induced Pluripotent Stem Cells form Calcified Structures in Scaffolds Both In Vitro and In Vivo. *Stem Cells*. 2011; 29:206-216.

Cheng Z, Alba-Perez A, Gonzalez-Garcia C, et al. Nanoscale Coatings for Ultralow Dose BMP‐2‐Driven Regeneration of Critical‐Sized Bone Defects. *Advanced Science*. 2018;1800361.

Chiaraviglio L, Kirby JE. Evaluation of impermeant, DNA-binding dye fluorescence as a real-time readout of eukaryotic cell toxicity in a high throughput screening format. *Assay Drug Dev Technol*. 2014;12(4):219-28.

Costa, Fabíola, et al. "Covalent immobilization of antimicrobial peptides (AMPs) onto biomaterial surfaces." *Acta biomaterialia.* 2011; 7(4): 1431-1440.

Dr. Biology. (2011, February 04). Bone Anatomy. ASU - Ask A Biologist. Retrieved December 5, 2018 from https://askabiologist.asu.edu/bone-anatomy

Fu C, Bai H, Hu Q, Gao T, Bai Y. "Enhanced proliferation and osteogenic differentiation of MC3T3-E1 pre-osteoblasts on graphene oxide-impregnated PLGA–gelatin nanocomposite fibrous membranes." *Royal Society of Chemistry*. 2016; 7:8886-8897.

Humblot, V., Yala, J. F., Thebault, P., Boukerma, K., Héquet, A., Berjeaud, J. M., & Pradier, C. M. (2009). The antibacterial activity of Magainin I immobilized onto mixed thiols Self-Assembled Monolayers. *Biomaterials*, *30*(21), 3503-3512.

Jariwala, Sahilly, et al., "3D Printing of Personalized Artificial Bone Scaffolds." *3D Printing and Additive Manufacturing* vol. 2 no. 2, pp. 56-64, 01 June 2015.

Kim MS, Jeong S, Lim HG, and Kim YK. Differences in xenoreactive immune response and patterns of calcification of porcine and bovine tissues in α-Gal knock-out and wild-type mouse implantation models. *European Journal of Cardiothoracic Surgery*. 2015: 48(3):392-398.

Kinaci, Ahmet, et al., "Trends in Bone Graft Use in the United States." *Orthopedics* vol. 37 no. 9, pp. 783-788, September 2014.

Lee, Fang-Hsin, et al., "A Population-Based 16-Year Study on the Risk Factors of Surgical Site Infection in Patients after Bone Grafting." *Medicine(Baltimore).* vol. 94 issue 47 November 2015.

Li, Yuanyuan, et al. "Fabrication of antimicrobial peptide-loaded PLGA/chitosan composite microspheres for long-acting bacterial resistance." *Molecules* 22.10 (2017): 1637.

Liu, Yi, et al. "The antimicrobial and osteoinductive properties of silver nanoparticle/poly (DL-lactic-co-glycolic acid)-coated stainless steel." *Biomaterials* 33.34 (2012): 8745-8756.

Llopis-Hernandez V, Cantini M, Gonzalez-Garcia C, Cheng Z, Yang J, Tsimbouri PM, Garcia AJ, Dalbu MJ, Salmeron-Sanchez M. "Material-driven fibronectin assembly for high-efficiency presentation of growth factors." *Science Advances*. 2016; 2(8):e1600188

Luo Y, Lode A, Sonntag F, Nies B, and Gelinsky M. Well-ordered biphasic calcium phosphate–alginate scaffolds fabricated by multi-channel 3D plotting under mild conditions. *Journal of Materials Chemistry B*. 2013; 1:4088-4098.

Martín, Cristina, et al., "Graphene improves the biocompatibility of polyacrylamide hydrogels: 3D polymeric scaffolds for neuronal growth." Scientific Reports vol. 7, pp. 1-12, 08 September 2017.

Nie B, Ao H, Long T, Zhou J, Tang T, Yue B. "Immobilizing bacitracin on titanium for prophylaxis of infections and for improving osteoinductivity: an *in vivo* study." *Colloids and Surfaces B: Biointerfaces*. 2017; 150:183-191.

Park S.H., Park D.S., Shin J.W., et al. 2012. "Scaffolds for bone tissue engineering fabricated from two different materials by the rapid prototyping technique: PCL versus PLGA". *Journal of Materials Science: Materials in Medicine.* 23(11): 2671-2678.

Qi, Ruiling, et al. "Controlled release and antibacterial activity of antibiotic-loaded electrospun halloysite/poly (lactic-co-glycolic acid) composite nanofibers." *Colloids and Surfaces B: Biointerfaces* 110 (2013): 148-155.

Wang L, Li ZY, Wang YP, Wu ZH, and Yu B. Dynamic Expression Profiles of Marker Genes in Osteogenic Differentiation of Human Bone Marrow-derived Mesenchymal Stem Cells. *Chinese Medical Sciences Journal.* 2015; 30(2):108-13.

Xu, Thomas, et al., "Self-neutralizing PLGA / Magnesium Composites as Novel Biomaterials for Tissue Engineering." *Biomaterials Materials* vol. 13, no. 3, pp. 1 – 12, 16 March 2018.

Yüksel, Emre, and Ayşe Karakeçili. "Antibacterial activity on electrospun poly (lactide-co-glycolide) based membranes via Magainin II grafting." Materials Science and Engineering: C 45 (2014): 510-518.

Yüksel, E., Karakeçili, A., Demirtaş, T. T., & Gümüşderelioğlu, M. (2016). Preparation of bioactive and antimicrobial PLGA membranes by magainin II/EGF functionalization. *International journal of biological macromolecules*, *86*, 162-168.

Zein, Iwan, et al., "Fused deposition modeling of novel scaffold architectures for tissue engineering applications." *Biomaterials* vol 23, no. 4, pp. 1169-1185, 15 February 2002.